—Original Article—

Runx3 transcription factor regulates ovarian functions and ovulation in female mice

Fumiya OJIMA[1)*], **Yuka SAITO**[1)*], **Yukiko TSUCHIYA**[1)], **Daichi KAYO**[1)], **Syusuke TANIUCHI**[1)], **Maho OGOSHI**[1)], **Hiroshi FUKAMACHI**[2)], **Sakae TAKEUCHI**[1)] and **Sumio TAKAHASHI**[1)]

[1)]*The Graduate School of Natural Science and Technology, Okayama University, Okayama 700-8530, Japan*
[2)]*The Graduate School of Medical and Dental Sciences, Tokyo Medical and Dental University, Tokyo 113-8519, Japan*

Abstract. We previously demonstrated that the Runx3 transcription factor is expressed in the hypothalami, pituitaries, and ovaries of mice, and that *Runx3* knockout (*Runx3*$^{-/-}$) mice are anovulatory and their uteri are atrophic. *Runx3* mRNA expression was detected in the granulosa cells of ovarian follicles, and in the anteroventral periventricular nucleus (AVPV) and arcuate nucleus (ARC). In the present study, we examined the effects of *Runx3* knockout on the gene expression of enzymes associated with steroidogenesis. We found decreased *Cyp11a1* mRNA expression in *Runx3*$^{-/-}$ mouse ovaries compared with that in wild-type (wt) mouse ovaries at the age of 8 weeks. *In situ* hybridization analysis showed that the percentages of *Cyp11a1* mRNA-expressing theca cells in follicles of *Runx3*$^{-/-}$ mice were decreased compared with those of wt mice. In accord with the alterations in *Runx3*$^{-/-}$ mouse ovaries, *Kiss1* mRNA levels in ARC were increased, whereas mRNA levels of kisspeptin in AVPV were decreased, and gonadotropin-releasing hormone in the preoptic area and follicle-stimulating hormone β subunit gene were increased in *Runx3*$^{-/-}$ mice. Following an ovarian transplantation experiment between *Runx3*$^{-/-}$ mice and wt mice, corpora lutea were observed when ovaries from *Runx3*$^{-/-}$ mice were transplanted into wt mice, but not when those from wt mice were transplanted into *Runx3*$^{-/-}$ mice, suggesting that Runx3 in the hypothalamo-pituitary system may drive gonadotropin release to induce ovulation in the ovary. These findings indicate that Runx3 plays a crucial role in the hypothalamo-pituitary-gonadal axis.
Key words: Mouse, Ovary, Ovulation, Steroidogenesis

(J. Reprod. Dev. 62: 479–486, 2016)

The runt domain transcription factors, also known as the polyoma-virus enhancer binding protein 2/core binding factors (PEBP2/CBF), are heterodimeric transcriptional regulators composed of α and β subunits [1–3]. The α subunit is required for binding with the consensus DNA sequence and for dimerization with the β subunit. The gene encoding the α subunit is homologous to the *Drosophila* gene *runt*, and three runt-related genes, *Runx1*, *Runx2*, and *Runx3*, have been identified. These Runx proteins interact with Smad2 or Smad3, and play an important role in transforming growth factor-β (TGF-β) superfamily signaling [4].

Runx3 functions as a tumor suppressor in a variety of cancers, including gastric and esophageal cancers [5, 6]. A previous study demonstrated that Runx3 functions as a tumor suppressor in the TGF-β signaling pathway through the attenuation of cell growth and the induction of apoptosis [7]. Runx3 suppresses gastric epithelial cell growth by inducing the expression of the cell cycle regulator $p21^{WAF1/Cip1}$ and induces apoptosis of gastric epithelial cells by enhanced expression of the pro-apoptotic gene *Bim*.

Runx1, Runx2, and Runx3 are involved in the regulation of ovarian functions. Runx1 and Runx2 play crucial roles in the periovulatory process of rat ovaries [8–11]. Recently, we revealed that expression of *Runx3* mRNA was observed in various mouse organs, including the hypothalami, pituitaries, ovaries, and uteri [12]. The ovaries of adult *Runx3* knockout (*Runx3*$^{-/-}$) mice were smaller than those of adult wild-type (wt) mice. Corpora lutea were not observed in *Runx3*$^{-/-}$ mouse ovaries, indicating a lack of ovulation. The numbers of primary, secondary, and antral follicles were significantly lower in *Runx3*$^{-/-}$ mouse ovaries than those in wt mouse ovaries, indicating that folliculogenesis was retarded. In addition, atrophic uteri were observed in *Runx3*$^{-/-}$ mice, suggesting a decrease in estrogen and progesterone (P4) production [12, 13]. However, it is not clear how *Runx3* deletion affects steroidogenesis in mouse ovaries.

Steroidogenesis in ovaries is regulated by follicle-stimulating hormone (FSH) and luteinizing hormone (LH). Estradiol (E2), in concert with the gonadotropins, acts on follicles to induce their growth and maturation [14]. To determine whether *Runx3* knockout affects steroidogenesis in mouse ovaries, we analyzed mRNA levels of *Fshr* (FSH receptor), *Lhcgr* (luteinizing hormone receptor), and the key regulators of steroidogenesis in ovarian granulosa cells: *Star* (steroidogenic acute regulatory protein), *Cyp11a1* (p450scc, cholesterol side chain cleavage enzyme), *Hsd3b1* (hydroxy-delta-5-steroid dehydrogenase), *Cyp17a1* (p450c17, steroid 17-alpha hydroxylase), and *Cyp19a1* (p450arom, aromatase) in wt and *Runx3*$^{-/-}$ mouse ovaries.

Ovulation is triggered by preovulatory gonadotropin-releasing hormone (GnRH)/LH surges on the evening of the proestrous day, and the GnRH/LH surge is generated by the positive feedback action of E2 through the stimulatory action of kisspeptin neurons in the anteroventral periventricular nucleus (AVPV) [15, 16]. Kisspeptin neurons in the arcuate nucleus (ARC) are involved in the negative feedback regulation of LH and FSH secretions [16, 17]. To investigate the effects of *Runx3* knockout on gonadotropin secretion, we analyzed mRNA levels of kisspeptin and GnRH genes in the preoptic area (POA)-AVPV and ARC areas using real-time PCR. In addition, to analyze contributions of the hypothalamo-pituitary system to the anovulation of *Runx3*$^{-/-}$ mice, we performed transplantation of ovaries obtained from *Runx3*$^{-/-}$ mice to wt or *Runx3*$^{-/-}$ mice, and then ovulation in grafted ovaries was examined by histological observation of grafts.

Materials and Methods

Animals

Male and female BALB/c mice were used in this study. *Runx3* knockout (*Runx3*$^{-/-}$) mice with the BALB/c genetic background were generated as previously described [18]. All animal care and experimentation was approved by the Animal Care and Use Committee, Okayama University, and was conducted in accordance with the Policy on the Care and Use of Laboratory Animals, Okayama University. *Runx3*$^{+/-}$ mice were mated, and the offspring were genotyped as previously described [12, 19].

Ovarian granulosa cell isolation

Granulosa cell isolation was performed according to a method described in a previous study [20]. Ovaries from 3-week-old wt mice were removed and dissected free of connective tissue. The ovaries were incubated in M199 medium (Sigma-Aldrich, St. Louis, MO, USA) containing 25 mM HEPES and 0.1% BSA, and were punctured with a 27-gauge needle. Mixtures of granulosa cells and oocytes were filtered through cell strainers (40-µm nylon mesh, BD Falcon, Bedford, MA, USA) that allowed granulosa cells but not oocytes to pass through. After centrifugation (5 min at 500 × *g* 4°C) cells were collected.

Brain sample and anterior pituitary sample collection

Whole brains of 8-week-old wt mice at the diestrous stage and *Runx3*$^{-/-}$ mice were rapidly removed from the skull and frozen in liquid nitrogen. Two parts, one containing the POA and AVPV and the other containing the ARC, were dissected from the frozen brain. Briefly, an anterior coronal cut was performed approximately 2 mm anteriorly from the anterior part of the optic chiasma, and a posterior coronal cut was performed at the posterior border of the mammillary bodies. The dissected brain sample was further coronally cut 1 mm behind the optic chiasma, dorsally at the upper portion of the third ventricle (approximately 2 mm from the ventral surface of the block), and laterally at the hypothalamic fissure.

Anterior pituitaries of 8-week-old wt mice at the diestrous stage and *Runx3*$^{-/-}$ mice were rapidly removed and frozen in liquid nitrogen.

Riboprobes

Mouse *Runx3*, *Cyp11a1*, and *Cyp19a1* riboprobes were generated according to a previously described method [21]. DNA fragments encoding part of mouse *Runx3* (NM_019732; 1770–2071), *Cyp11a1* (NM_019779.3; 630–1055), and *Cyp19a1* (NM_007810.3; 286–789) were obtained by reverse transcription-polymerase chain reaction (RT-PCR) using the following primers: mouse *Runx3*: 5′-CTC CAG CCC GAG ACT ACA AG-3′ and 5′-AGG GAG GGA GAG AAA GTC CA-3′; mouse *Cyp11a1*: 5′-CCT TTG AGT CCA TCA GCA GTG-3′ and 5′-GTA CCT TCA AGT TGT GTG CCA-3′; mouse *Cyp19a1*: 5′-GAG AGT TCA TGA GAG TCT GG-3′ and 5′-CCT TGA CGG ATC GTT CAT AC-3′. The cDNA fragments were subcloned into the pGEM-3zf(+) vector. Each plasmid DNA was linearized using restriction enzyme (*Eco*RI/*Hin*dIII) sites of pGEM-3Zf(+) and RNA probes were synthesized using a T7 and SP6 polymerase system (Promega, Madison, WI, USA) according to the manufacturer's instructions. The probe was labeled with digoxigenin (DIG) (Roche Diagnostics, Mannheim, Germany).

In situ hybridization analysis

Ovaries from wt and *Runx3*$^{-/-}$ mice were embedded in O.C.T. Compound (Sakura Finetek Japan, Tokyo, Japan), frozen with liquid nitrogen, and sectioned at 10-µm thickness using a cryostat. The dried sections were treated with 0.5 µg/ml proteinase K (Nacalai Tesque, Kyoto, Japan) at 37°C for 10 min and 0.2% glycine in PBS for 20 min, and then acetylated with 0.15 M acetic anhydride in 0.1 M triethanolamine for 10 min at room temperature. The sections were then treated with pre-hybridization solution containing 4 × SSPE, 1 × Denhardt's solution, 10% dextran sulfate, 50% deionized formamide, and yeast tRNA (50 µg/slide) at room temperature for 30 min. After pre-hybridization, the sections were subjected to hybridization solution containing DIG-labeled anti-sense or sense riboprobes (50 ng/slide) in pre-hybridization solution overnight at 53°C (*Runx3*) or 45°C (*Cyp11a1* and *Cyp19a1*). Following hybridization for 16 h, the sections were incubated with alkaline phosphatase (AP)-conjugated anti-DIG-antibody (Roche Diagnostics) in blocking solution overnight at 4°C. Hybridization signals were detected in AP buffer containing 35 µg/ml nitro-blue tetrazolium chloride (Wako Pure Chemical, Osaka, Japan) and 17.5 µg/ml 5-bromo-4-chloro-3′-indoylphosphate *p*-toluidine salt (Wako Pure Chemical). To evaluate the effect of *Runx3* deletion on *Cyp11a1* mRNA expressions, follicles in medial sections of serial ovarian sections were selected from five wt mice and three *Runx3*$^{-/-}$ mice, and both identifiable *Cyp11a1* mRNA-expressing theca cells and all theca cells were counted by light microscopy. Data are expressed as the percentage of the number of *Cyp11a1* mRNA-expressing theca cells against total number of theca cells.

RNA extraction and reverse transcription (RT)-polymerase chain reaction (PCR)

Total RNA was extracted from tissues using TRIsure Reagent (Bioline, London, UK), and reverse-transcribed using the Prime Script RT-PCR System (Takara Bio) according to the manufacturer's instructions. Random hexamers were used for the RT reactions. PCR was performed using Blend Taq (Toyobo, Tokyo, Japan) and a Gene Amp PCR System 9700 thermal cycler (Applied Biosystems, Branchburg, NJ, USA). The PCR conditions were as follows: 2

min at 94°C; an appropriate number of cycles of 94°C for 30 sec, annealing temperature for 30 sec, and 72°C for 30 sec; and 10 min at 72°C. A 10-μl aliquot of each reaction was electrophoresed on a 2% agarose gel, and the gel was stained with ethidium bromide and photographed under ultraviolet light.

Real-time PCR was performed using SYBR Premix Ex Taq (Perfect Real Time; Takara Bio) with an ABI PRISM 7300 Sequence Detection System (Applied Biosystems). The PCR program was as follows: an initial denaturing at 95°C for 10 sec, 40 cycles 95°C for 5 sec, and 60°C for 31 sec, followed by a melting-curve analysis (95°C for 15 sec, 60°C for 1 min, 95°C for 15 sec, 60°C for 15 sec). Melting curve analysis was conducted to confirm the absence of primer dimers. The primers used in this study are summarized in Table 1. Standard curves were generated by serial dilution of total cDNA, and the amount of each target mRNA level was normalized against the amount of ribosomal protein L19 (*Rpl19*) mRNA levels.

Ovarian transplantation

Ovary collection and transplantations were performed simultaneously. *Runx3*$^{-/-}$ and wt mice were ovariectomized under light anesthesia, and their ovaries were pulled out from a dorsal incision and were removed from the bursa surrounding the ovaries. Collected ovaries were maintained in M199 medium containing 25 mM HEPES and 0.1% bovine serum albumin (BSA, Sigma-Aldrich) at room temperature until transplantation. After ovariectomy, one ovary was immediately placed subcutaneously on the left ventral side of *Runx3*$^{-/-}$ and wt mice. Ovarian transplantation experiments were carried out as follows: wt ovaries were grafted to wt mice (designated as wt-wt); *Runx3*$^{-/-}$ ovaries were grafted to wt mice (*Runx3*$^{-/-}$-wt); wt ovaries were grafted to *Runx3*$^{-/-}$ mice (wt-*Runx3*$^{-/-}$); *Runx3*$^{-/-}$ ovaries were grafted to *Runx3*$^{-/-}$ mice (*Runx3*$^{-/-}$-*Runx3*$^{-/-}$). Nine- to ten-week-old wt and *Runx3*$^{-/-}$ mice received ovarian grafts from mice of the same age. In the transplantation of wt-*Runx3*$^{-/-}$ mice, ovaries from 4-week-old wt mice were grafted to *Runx3*$^{-/-}$ mice, since ovulation did not occur at the age of 4 weeks. To evaluate the number of estrous cycles, vaginal smears were checked for 17 consecutive days during pre-transplantation and post-transplantation periods. The estrous cycle was classified into the following four phases: proestrus, estrus, metoestrus, and diestrus. Ovarian grafts were collected 17 days after transplantation, and processed for histological observation.

Statistical analysis

The differences in means between the two groups were analyzed using Student's *t*-test (Kaleida Graph, Synergy Software, Reading, PA, USA). The differences were considered significant at P < 0.05.

Results

Expression of Runx3 mRNA in granulosa cells and hypothalami in female mice

Granulosa cells were isolated from the ovaries of 3-week-old mice, and were confirmed by detection of the expression of *Fshr* and *Cyp19a1* (Fig. 1A). *Runx3* mRNA was detected in the isolated granulosa cells by RT-PCR. *Runx3* mRNA expression in the AVPV and ARC of 8-week-old wt female mice at diestrus was analyzed

by real-time PCR. *Runx3* mRNA was detected in both areas as well as in granulosa cells (Fig. 1B). *Runx3* mRNA expression in ovaries was verified by *in situ* hybridization (Fig. 1C, E). *Runx3* mRNA hybridization signals were detected in the granulosa cells of antral follicles. No signals were detected with the sense probe (Fig. 1D, F).

Expression of genes involved in regulation of steroidogenesis in the ovaries of wt and Runx3$^{-/-}$ mice

To determine whether *Runx3* deletion can affect steroidogenesis in 8-week-old mouse ovaries, we analyzed the mRNA levels of *Fshr*, *Lhcgr*, *Star*, *Cyp11a1*, *Hsd3b1*, *Cyp17a1*, and *Cyp19a1* in wt and *Runx3*$^{-/-}$ mouse ovaries using real-time PCR. Wt mice at the diestrous stage, and *Runx3*$^{-/-}$ mice showing acyclic state and diestrous vaginal smear, were selected for the analysis. *Cyp11a1* mRNA levels in *Runx3*$^{-/-}$ mouse ovaries were lower than those in wt mice. There were no differences in the mRNA levels of *Fshr*, *Lhcgr*, *Star*, *Hsd3b1*, *Cyp17a1*, and *Cyp19a1* between wt and *Runx3*$^{-/-}$ mice (Fig. 2).

In situ hybridization analysis of Cyp11a1 and Cyp19a1 mRNA expression in wt and Runx3$^{-/-}$ mouse ovaries

Cyp11a1 and *Cyp19a1* mRNA expressions in 8-week-old mice were analyzed using DIG-labeled riboprobes. In all *in situ* hybridization studies, no signals were detected when sense riboprobes were used as the control analysis.

Cyp11a1 mRNA: In wt mice, *Cyp11a1* mRNA signals were detected in the interstitial cells and theca interna cells of secondary and antral follicles. In preovulatory antral follicles, granulosa cells that were located near the follicular basement membrane expressed *Cyp11a1* mRNA signals, but the cells surrounding an oocyte did not (Fig. 3A, C). Intense signals were detected in the corpora lutea (Fig. 3A). In *Runx3*$^{-/-}$ mice, *Cyp11a1* mRNA signals were detected in interstitial cells and theca interna cells, but the number of *Cyp11a1* mRNA-containing cells was lower than that in wt mice (Fig. 3B, D, G). No signals were detected with the sense probe (Fig. 3E, F).

Cyp19a1 mRNA: In wt mice, *Cyp19a1* mRNA signals were detected in the granulosa cells of antral follicles in both wt and *Runx3*$^{-/-}$ mice (Fig. 4A, B). *Cyp19a1* mRNA expressions in granulosa cells did not differ between wt and *Runx3*$^{-/-}$ mice (Fig. 4C, D). These results were consistent with the results obtained from quantitative real-time PCR analyses (Fig. 2). No signals were detected with the sense probe (Fig. 4E, F).

Expression of Gnrh1, Kiss1, Cga, Fshb, and Lhb mRNA in wt and Runx3$^{-/-}$ mice

To clarify alterations of the hypothalamo-pituitary system in *Runx3*$^{-/-}$ mice, mRNA levels of GnRH, kisspeptin, FSH, and LH genes were analyzed by real-time PCR. *Gnrh1* mRNA levels were significantly higher than those in wt mice (Fig. 5A). *Kiss1* mRNA levels in AVPV in *Runx3*$^{-/-}$ mice were significantly lower than those in wt mice (Fig. 5B), whereas *Kiss1* mRNA levels in ARC were significantly higher than those in wt mice (Fig. 5B). In addition, estrogen receptor α (*Esr1*) mRNA levels were determined by real-time PCR, and did not differ between the POA-AVPV and ARC of wt and *Runx3*$^{-/-}$ mice (data not shown). *Fshb* mRNA levels in anterior pituitaries were significantly higher in *Runx3*$^{-/-}$ mice than those in wt

Table 1. Primers used for RT-PCR and real-time PCR

For RT-PCR

Gene		5' - sequence - 3'	Tm (°C)	Product (bp)
Runx3	FP	AAGTGCGCTCGATGGTGGACG	65	369
	RP	CAGTGACCTTGATGGCTCGGT		
Fshr	FP	GGAGGCGGCAAACCTCTGAA	60	350
	RP	CCGGGGCACAGTGAGTTTGT		
Lhcgr	FP	GAGAAGCGAATAACGAGACGCT	60	338
	RP	TTGGGAGTCTACTGAGGCAATG		
Cyp11a1	FP	CCTTTGAGTCCATCAGCAGTG	60	426
	RP	GTACCTTCAAGTTGTGTGCCA		
Hsd3b1	FP	CAGGAGCAGGAGGGTTTGT	55	391
	RP	GTGGCCATTCAGGACGAT		
Cyp17a1	FP	CTGCTCATCCTGGCCTATTTCTTT	55	562
	RP	TAGTCAGTATCGGATCCTTGTTCT		
Cyp19a1	FP	GAGAGTTCATGAGAGTCTGG	55	504
	RP	CCTTGACGGATCGTTCATAC		
Rpl19	FP	GAAATCGCCAATGCCAACTC	60	406
	RP	TCTTAGACCTGCGAGCCTCA		

For real-time PCR

Gene				
Runx3	FP	GCCGGCAATGATGAGAACTA		250
	RP	AGGCCTTGGTCTGGTCTTCTAT		
Fshr	FP	AGCAAGTTTGGCTGTTATGAGG		159
	RP	GTTCTGGACTGAATGATTTAGAGG		
Lhcgr	FP	CCTTGTGGGTGTCAGCAGTTAC		75
	RP	TTGTGACAGAGTGGATTCCACAT		
Star	FP	GACGTCGGAGCTCTCTGCTT		100
	RP	GCCTTCTGCATAGCCACCTC		
Cyp11a1	FP	ACATGGCCAAGATGGTACAGTTG		121
	RP	ACGAAGCACCAGGTCATTCAC		
Hsd3b1	FP	CTCAGTTCTTAGGCTTCAGCAATTAC		101
	RP	CCAAAGGCAGGATATGATTTAGGA		
Cyp17a1	FP	GATCTAAGAAGCGCTCAGGCA		69
	RP	GGGCACTGCATCACGATAAA		
Cyp19a1	FP	AACCCGAGCCTTTGGAGAA		57
	RP	GGCCCGTCAGAGCTTTCA		
Gnrh1	FP	ACTGCTGACTGTGTGTTTGGAAG		120
	RP	GTAGAAGAGGTGTGAAGACGACATG		
Kiss1	FP	TGATCTCAATGGCTTCTTGGCAGC		154
	RP	CTCTCTGCATACCGCGATTCCTTT		
Cga	FP	CCACCTCCTCCCTACCAGACT		62
	RP	TGTAACCGTAAAGAGGCAGTGTGT		
Fshb	FP	TGGATTGTTCCAGGCAGACA		70
	RP	GGTGGCAATACCTTGGGAAA		
Lhb	FP	CCCTTGGTCTCCCATTTCTG		67
	RP	TGCTGGTGAGATGCCAGTTG		
Rpl19	FP	CCCGTCAGCAGATCAGGAA		58
	RP	GTCACAGGCTTGCGGATGA		

FP: forward primer, RP: reverse primer.

mice. In contrast, *Lhb* and *Cga* mRNA levels in anterior pituitaries did not differ between *Runx3*$^{-/-}$ and wt mice (Fig. 5C).

Evaluation of contribution of the hypothalamo-pituitary system or ovaries to the anovulatory status of Runx3$^{-/-}$ *mice assessed by ovarian transplantation*

To study the contribution of the hypothalamo-pituitary system or ovaries to the anovulatory status of *Runx3*$^{-/-}$ mice, we carried out reciprocal ovarian transplantation between *Runx3*$^{-/-}$ and wt mice, and monitored vaginal smears for 17 consecutive days before and after the transplantation. The experimental grafts were conducted as follows: wt ovaries were grafted to wt mice (designated as wt-wt); *Runx3*$^{-/-}$ ovaries were grafted to wt mice (*Runx3*$^{-/-}$-wt); wt ovaries were grafted to *Runx3*$^{-/-}$ mice (wt-*Runx3*$^{-/-}$); and *Runx3*$^{-/-}$ ovaries were grafted to *Runx3*$^{-/-}$ mice (*Runx3*$^{-/-}$-*Runx3*$^{-/-}$). Before the ovarian transplantation, wt mice exhibited regular cyclic estrous cycles, whereas *Runx3*$^{-/-}$ mice had irregular or acyclic estrous cycles. After the ovarian transplantation, there was no difference in the number of estrous cycles during the observation period (17 days) between *Runx3*$^{-/-}$-wt mice (2.17 ± 0.31) and wt-wt mice (2.20 ± 0.20). In contrast, in wt-*Runx3*$^{-/-}$ mice (0.40 ± 0.24, P < 0.001) and *Runx3*$^{-/-}$-*Runx3*$^{-/-}$ mice (0, P < 0.001), the number of the cycles was significantly lower than that in wt-wt mice.

The presence of corpora lutea in ovarian grafts was assessed as an indication of ovulation. Corpora lutea were detected in ovarian grafts collected from wt-wt mice (Fig. 6A, E), but were not detected in ovarian grafts collected from *Runx3*$^{-/-}$-*Runx3*$^{-/-}$ mice (Fig. 6B, F). In spite of the lack of corpora lutea in ovaries of *Runx3*$^{-/-}$ mice, numerous antral follicles and corpora lutea were detected in ovarian grafts collected from *Runx3*$^{-/-}$-wt mice (Fig. 6C, G). However, although there were no corpora lutea in the ovarian grafts from wt-*Runx3*$^{-/-}$ mice, antral follicles were observed (Fig. 6D, H).

Discussion

The present study showed that *Runx3* mRNA was expressed in the granulosa cells of ovarian follicles, and in the AVPV and ARC areas of female mice, and that *Runx3* deletion decreased *Cyp11a1* mRNA expression in mouse ovaries. Furthermore, *Gnrh1* and *Kiss1* mRNA expressions were affected in *Runx3*$^{-/-}$ mice. The significant decrease in *Cyp11a1* mRNA levels in *Runx3*$^{-/-}$ mouse ovaries may result in decreased androgen synthesis, leading to the diminished production of estrogen in granulosa cells. Atrophic uteri in *Runx3*$^{-/-}$ mice also suggested a decrease in estrogen production in ovaries [13]. The increase in estrogen levels during the proestrous day triggers a preovulatory GnRH/LH surge. Therefore, it is probable that anovulation of *Runx3*$^{-/-}$ mice was caused by a decrease in estrogen production from granulosa cells, or by alterations in the preovulatory GnRH/LH surge-generating system in the hypothalamus of *Runx3*$^{-/-}$ mice. In the present study, ovulation was induced in the ovaries of *Runx3*$^{-/-}$ mice when they were transplanted into wt mice. These results indicate that *Runx3*$^{-/-}$ mouse ovaries are able to respond to gonadotropins and then to release oocytes, and that dysfunction of the hypothalamo-pituitary system in *Runx3*$^{-/-}$ mice is closely associated with anovulation.

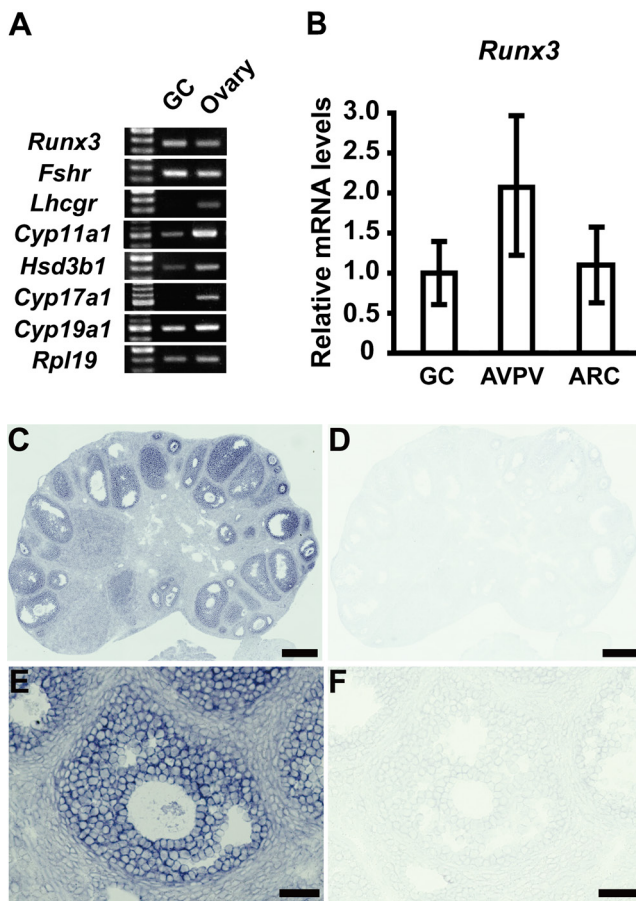*Cyp11a1* encodes the cholesterol side chain cleavage enzyme

Fig. 1. Expression of *Runx3* mRNA in granulosa cells (GCs) and hypothalami of female mice. GCs were isolated from the ovaries of 3-week-old mice. The expressions of *Runx3, Fshr, Lhcgr, Cyp11a1, Hsd3b1, Cyp17a1,* and *Cyp19a1* mRNA were analyzed in the GCs and whole ovaries of 3-week-old mice (A). Expression of *Runx3* mRNA levels in 3-week-old wt mouse GCs and in the POA-AVPV and ARC of 8-week-old wt mouse hypothalami (B). *In situ* hybridization analysis detected *Runx3* mRNA signals in the GCs of 8-week-old mouse ovaries (C, E). No signals were detected when a sense probe was used (D, F). Bar = 300 μm (C, D), 50 μm (E, F).
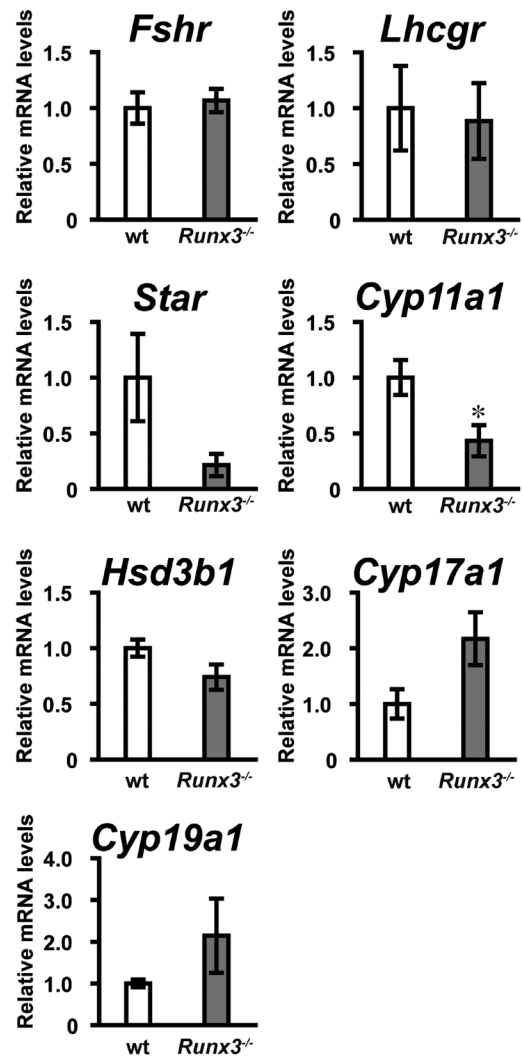
Fig. 2. Expression of gonadotropin receptor, steroidogenic acute regulatory protein (StAR), and steroidogenic enzymes in the whole ovary of wt and *Runx3⁻/⁻* mice at the age of 8 weeks. Real-time PCR was performed for quantitative analysis of *Fshr, Lhcgr, Star, Cyp11a1, Hsd3b1, Cyp17a1,* and *Cyp19a1* mRNA expression. The amount of each mRNA in wt and *Runx3⁻/⁻* mice was normalized against that of *Rpl19* mRNA. Each group consisted of five mice. Data are expressed as the mean ± SEM of triplicate wells. * P < 0.05, significantly different from wt mice.

(SCC), which is a key enzyme catalyzing the rate-limiting step in the synthesis of steroid hormones in ovaries. *In situ* hybridization analysis showed that *Cyp11a1* mRNA was expressed in theca interna cells, some of the granulosa cells in preovulatory follicles, and corpora lutea, which is in agreement with a previous study [22]. We found decreased expression of *Cyp11a1* mRNA in *Runx3⁻/⁻* mouse whole ovaries, and a decrease in the percentage of identifiable *Cyp11a1* mRNA-expressing cells in the theca cell layers of *Runx3⁻/⁻* mouse ovaries, possibly resulting from the decrease in *Cyp11a1* mRNA expression in theca cells.

The decreased expression of *Cyp11a1* mRNA may affect the whole process of ovarian steroidogenesis, although *Hsd3b1* and *Cyp19a1* mRNA levels in *Runx3⁻/⁻* mouse ovaries did not change. Estrogen is a final product of the steroidogenesis of granulosa cells, and is closely

related to the progress of folliculogenesis, onset of ovulation, and uterine growth and functions [14]. Defects in the female reproductive system observed in *Runx3⁻/⁻* mice, such as retarded folliculogenesis, anovulation, and atrophied uteri [12], may be attributable to estrogen deficiency. Therefore, Runx3 is one of the key transcription factors involved in the regulation of ovarian functions.

In the present study, *Runx3* mRNA expression was detected in granulosa cells, but not in theca cells. *Cyp11a1* expression in the theca cells is regulated not only by LH [23], but also by growth factors produced in granulosa cells [24]. Therefore, the decreased *Cyp11a1* mRNA expression in theca cells may result from a disorder of LH
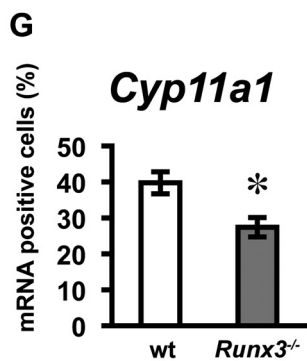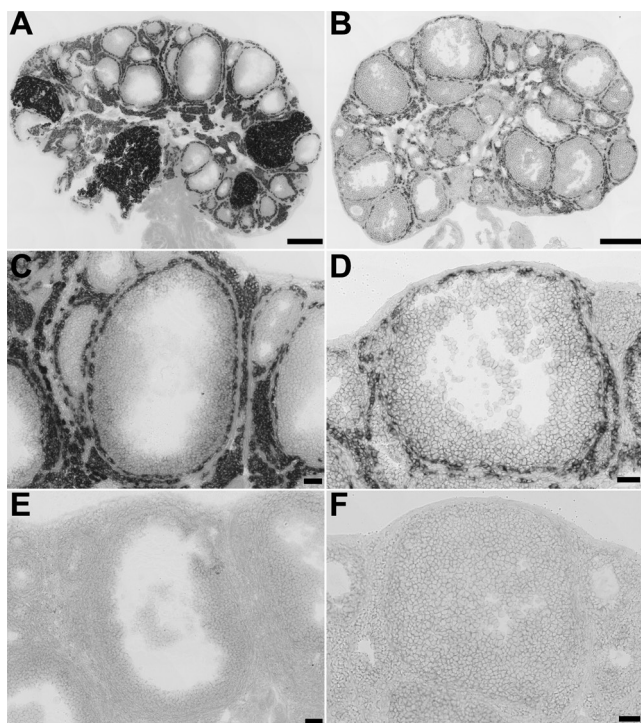
Fig. 4. *In situ* hybridization analysis of *Cyp19a1* mRNAs in ovaries from wt and *Runx3*^{−/−} mice at 8 weeks of age. Ovarian sections were obtained from wt and *Runx3*^{−/−} mice. DIG-labeled anti-sense riboprobes for *Cyp19a1* and sense probes were used. *Cyp19a1* mRNA signals were detected in granulosa cells (C, D). No signals were detected when the sense probe was used for hybridization (E, F). Bar = 300 μm (A, B), 50 μm (C–F).

Fig. 3. *In situ* hybridization analysis of *Cyp11a1* mRNAs in ovaries from wt and *Runx3*^{−/−} mice at 8 weeks of age. Ovarian sections were obtained from wt mice (A, C, E) and *Runx3*^{−/−} mice (B, D, F). DIG-labeled anti-sense riboprobes for *Cyp11a1* and sense probes were used. *Cyp11a1* mRNA signals were detected in theca cells (C, D). No signals were detected when a sense probe was used for hybridization (E, F). Quantitative analysis of *Cyp11a1* mRNA-positive theca cells in ovaries from wt and *Runx3*^{−/−} mice was performed, and the percentage of *Cyp11a1* mRNA-positive cells in theca cells was calculated (G). * P < 0.05, significantly different from wt mice. Bar = 300 μm (A, B), 50 μm (C–F).

secretion induced by *Runx3* deletion, and/or alterations in granulosa cell functions relating to the control of theca cell functions. Inhibin and activin, both produced in granulosa cells, stimulate and inhibit androgen synthesis in theca cells, respectively [25, 26]. Interestingly, a recent report suggests that *Inhbb*, which is one of the inhibin subunit genes, is involved in the regulation of *Cyp11a1* expression in mouse ovaries [27]. IGF1, produced in granulosa cells, regulates androgen production through stimulation of *Cyp11a1* and *Hsd3b1*
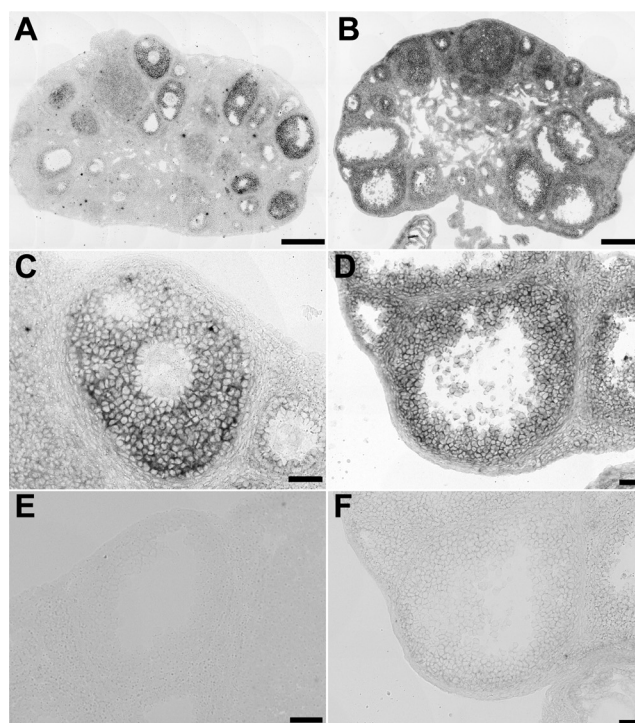
expression [23, 28, 29]. Considering these findings, it is probable that the decreased *Cyp11a1* mRNA expression in *Runx3*^{−/−} mouse ovaries is partly caused by altered production of growth factors in granulosa cells. Studies on such theca-granulosa cell interaction in *Runx3*^{−/−} mouse ovaries are needed.

In a previous study, *Runx3* mRNA expression was detected in the mouse hypothalamus [12]. The present study more clearly demonstrated *Runx3* mRNA expression in the AVPV and ARC of the female mouse hypothalamus, suggesting that Runx3 may play roles in neuronal system regulation in both AVPV and ARC areas, although the identity of the *Runx3* mRNA-expressing cells has not been determined. Concurrent increase in *Gnrh1* and *Fshb* mRNA levels in *Runx3*^{−/−} mice indicates that FSH production was increased by enhanced GnRH release. GnRH release is well known to be regulated by kisspeptin neurons in the AVPV and ARC. ARC kisspeptin neurons are involved in regulation of the negative feedback system of FSH and LH secretion [16, 17, 30, 31]. Therefore, if the negative feedback system of gonadotropin secretion in ARC functions properly, low estrogen level may stimulate *Kiss1* mRNA expression in the ARC, leading to the stimulation of GnRH release. In the present study, we observed elevation of *Kiss1* mRNA levels in the ARC in *Runx3*^{−/−} mice. Considering these observations, it is concluded that Runx3 in the ARC may not be involved in the negative feedback
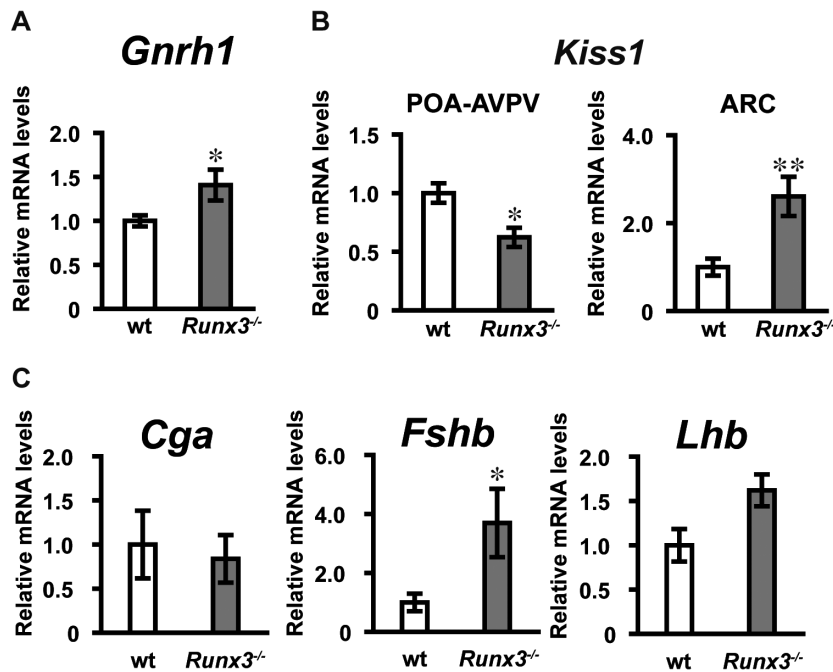
Fig. 5. *Gnrh1* and *Kiss1* mRNA levels and pituitary *Cga*, *Fshb*, and *Lhb* mRNA levels in wt and *Runx3*$^{-/-}$ mice at 8 weeks of age. * P < 0.05, ** P < 0.01, significantly different from wt mice.
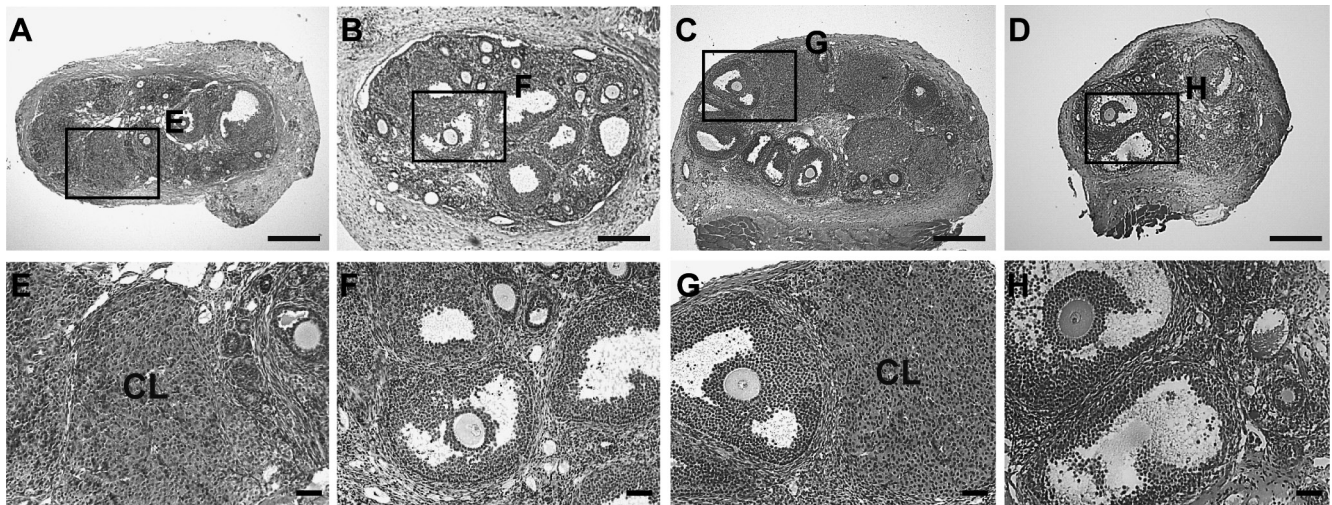

Fig. 6. Histological evaluation of ovarian transplantation. Ovarian transplantation was performed using 9- to 10-week-old *Runx3*$^{-/-}$ and wt mice according to the procedure described in the Material and Methods. Ovarian grafts were collected from wt-wt (A, E), *Runx3*$^{-/-}$-*Runx3*$^{-/-}$ (B, F), *Runx3*$^{-/-}$-wt (C, G), wt-*Runx3*$^{-/-}$ (D, H) mice 17 days after transplantation, and processed for histological observation. The boxed areas depicted in A, B, C, D correspond to the areas shown in E, F, G, H, respectively. CL: corpora lutea. Bar = 300 μm (A–D) and 20 μm (E–H).

system of *Kiss1* mRNA expression in the ARC.

Ovarian transplantation into wt or *Runx3*$^{-/-}$ mice was performed in order to determine whether the hypothalamo-pituitary system in *Runx3*$^{-/-}$ mice is impaired in regulation of ovulation, or whether *Runx3*$^{-/-}$ mouse ovaries loses the ability to ovulate. Wt mice bearing *Runx3*$^{-/-}$ ovarian grafts exhibited regular estrous cycles like wt mice bearing wt ovarian grafts, whereas *Runx3*$^{-/-}$ mice bearing wt ovarian

grafts exhibited irregular estrous cycles. With regard to formation of corpora lutea in ovarian grafts, ovarian grafts contained many corpora lutea in wt mice bearing *Runx3*$^{-/-}$ ovarian grafts, but not in *Runx3*$^{-/-}$ mice bearing wt ovarian grafts. These findings demonstrate that corpora lutea were observed in the ovaries of *Runx3*$^{-/-}$ mice when the ovaries were located in the hormonal milieu of wt mice, and hence ovulation was induced. In contrast, the hypothalamo-pituitary

system of *Runx3*⁻/⁻ mice failed to generate the GnRH/LH surge that induces ovulation, because corpora lutea were not detected in the ovaries of wt mice when they were transplanted into *Runx3*⁻/⁻ mice. Thus, these findings suggest that the ovaries in *Runx3*⁻/⁻ mice had the ability to produce E2 and undergo ovulation, and that anovulation in *Runx3*⁻/⁻ mice was caused by *Runx3* deletion in the hypothalamo-pituitary system leading to a probable alteration of gonadotropin secretion. This is consistent with our recent finding that gonadotropin treatment in 3-week-old *Runx3*⁻/⁻ mice induced ovulation, suggesting that the ovaries of *Runx3*⁻/⁻ mice could respond to gonadotropins and ovulate [12]. In *Runx3*⁻/⁻ mice, antral follicles were present in ovaries and the mRNA levels of *Gnrh1* in hypothalami and *Fshb* in anterior pituitaries were increased, suggesting that Runx3 in the hypothalamo-pituitary system is involved in LH surge release. Although expression of *Kiss1* mRNA in the AVPV and *Lhb* mRNA in the anterior pituitary were observed in *Runx3*⁻/⁻ mice, it remains unclear whether positive feedback and LH secretion are normal occurrences in these mice. The role of Runx3 in the hypothalamo-pituitary system remains to be studied.

In conclusion, Runx3 plays a pivotal role in the hypothalamo-pituitary-gonadal axis. Within the hypothalamo-pituitary system, Runx3 is involved in gonadotropin release, which induces steroidogenesis, and subsequently follicular maturation and ovulation in the ovary.

Acknowledgments

References

1. **Ito Y.** Molecular basis of tissue-specific gene expression mediated by the runt domain transcription factor PEBP2/CBF. *Genes Cells* 1999; **4**: 685–696. [Medline] [CrossRef]
2. **Otto F, Lübbert M, Stock M.** Upstream and downstream targets of RUNX proteins. *J Cell Biochem* 2003; **89**: 9–18. [Medline] [CrossRef]
3. **Cameron ER, Neil JC.** The Runx genes: lineage-specific oncogenes and tumor suppressors. *Oncogene* 2004; **23**: 4308–4314. [Medline] [CrossRef]
4. **Hanai J, Chen LF, Kanno T, Ohtani-Fujita N, Kim WY, Guo WH, Imamura T, Ishidou Y, Fukuchi M, Shi MJ, Stavnezer J, Kawabata M, Miyazono K, Ito Y.** Interaction and functional cooperation of PEBP2/CBF with Smads. Synergistic induction of the immunoglobulin germline Calpha promoter. *J Biol Chem* 1999; **274**: 31577–31582. [Medline] [CrossRef]
5. **Torquati A, O'rear L, Longobardi L, Spagnoli A, Richards WO, Daniel Beauchamp R.** RUNX3 inhibits cell proliferation and induces apoptosis by reinstating transforming growth factor beta responsiveness in esophageal adenocarcinoma cells. *Surgery* 2004; **136**: 310–316. [Medline] [CrossRef]
6. **Ito K, Liu Q, Salto-Tellez M, Yano T, Tada K, Ida H, Huang C, Shah N, Inoue M, Rajnakova A, Hiong KC, Peh BK, Han HC, Ito T, Teh M, Yeoh KG, Ito Y.** RUNX3, a novel tumor suppressor, is frequently inactivated in gastric cancer by protein mislocalization. *Cancer Res* 2005; **65**: 7743–7750. [Medline]
7. **Subramaniam MM, Chan JY, Yeoh KG, Quek T, Ito K, Salto-Tellez M.** Molecular pathology of RUNX3 in human carcinogenesis. *Biochim Biophys Acta* 2009; **1796**: 315–331. [Medline]
8. **Jo M, Curry TE Jr.** Regulation of matrix metalloproteinase-19 messenger RNA expression in the rat ovary. *Biol Reprod* 2004; **71**: 1796–1806. [Medline] [CrossRef]
9. **Jo M, Curry TE Jr.** Luteinizing hormone-induced RUNX1 regulates the expression of genes in granulosa cells of rat periovulatory follicles. *Mol Endocrinol* 2006; **20**: 2156–2172. [Medline] [CrossRef]
10. **Hernandez-Gonzalez I, Gonzalez-Robayna I, Shimada M, Wayne CM, Ochsner SA, White L, Richards JS.** Gene expression profiles of cumulus cell oocyte complexes during ovulation reveal cumulus cells express neuronal and immune-related genes: does this expand their role in the ovulation process? *Mol Endocrinol* 2006; **20**: 1300–1321. [Medline] [CrossRef]
11. **Park ES, Lind AK, Dahm-Kähler P, Brännström M, Carletti MZ, Christenson LK, Curry TE Jr, Jo M.** RUNX2 transcription factor regulates gene expression in luteinizing granulosa cells of rat ovaries. *Mol Endocrinol* 2010; **24**: 846–858. [Medline] [CrossRef]
12. **Sakuma A, Fukamachi H, Ito K, Ito Y, Takeuchi S, Takahashi S.** Loss of Runx3 affects ovulation and estrogen-induced endometrial cell proliferation in female mice. *Mol Reprod Dev* 2008; **75**: 1653–1661. [Medline] [CrossRef]
13. **Tsuchiya Y, Saito Y, Taniuchi S, Sakuma A, Maekawa T, Fukamachi H, Takeuchi S, Takahashi S.** Runx3 expression and its roles in mouse endometrial cells. *J Reprod Dev* 2012; **58**: 592–598. [Medline] [CrossRef]
14. **Drummond AE.** The role of steroids in follicular growth. *Reprod Biol Endocrinol* 2006; **4**: 16. [Medline] [CrossRef]
15. **Kinoshita M, Tsukamura H, Adachi S, Matsui H, Uenoyama Y, Iwata K, Yamada S, Inoue K, Ohtaki T, Matsumoto H, Maeda K.** Involvement of central metastin in the regulation of preovulatory luteinizing hormone surge and estrous cyclicity in female rats. *Endocrinology* 2005; **146**: 4431–4436. [Medline] [CrossRef]
16. **Smith JT, Cunningham MJ, Rissman EF, Clifton DK, Steiner RA.** Regulation of Kiss1 gene expression in the brain of the female mouse. *Endocrinology* 2005; **146**: 3686–3692. [Medline] [CrossRef]
17. **Dubois SL, Acosta-Martínez M, DeJoseph MR, Wolfe A, Radovick S, Boehm U, Urban JH, Levine JE.** Positive, but not negative feedback actions of estradiol in adult female mice require estrogen receptor α in kisspeptin neurons. *Endocrinology* 2015; **156**: 1111–1120. [Medline] [CrossRef]
18. **Li QL, Ito K, Sakakura C, Fukamachi H, Inoue K, Chi XZ, Lee KY, Nomura S, Lee CW, Han SB, Kim HM, Kim WJ, Yamamoto H, Yamashita N, Yano T, Ikeda T, Itohara S, Inazawa J, Abe T, Hagiwara A, Yamagishi H, Ooe A, Kaneda A, Sugimura T, Ushijima T, Bae SC, Ito Y.** Causal relationship between the loss of RUNX3 expression and gastric cancer. *Cell* 2002; **109**: 113–124. [Medline] [CrossRef]
19. **Yamamoto H, Ito K, Kawai M, Murakami Y, Bessho K, Ito Y.** Runx3 expression during mouse tongue and palate development. *Anat Rec A Discov Mol Cell Evol Biol* 2006; **288**: 695–699. [Medline] [CrossRef]
20. **Otsuka F, Shimasaki S.** A negative feedback system between oocyte bone morphogenetic protein 15 and granulosa cell kit ligand: its role in regulating granulosa cell mitosis. *Proc Natl Acad Sci USA* 2002; **99**: 8060–8065. [Medline] [CrossRef]
21. **Murakami Y, Otsuki M, Kusumoto K, Takeuchi S, Takahashi S.** Expression of interleukin-18 receptor mRNA in the decidualization of mouse uteri. *Zoolog Sci* 2005; **22**: 1504.
22. **Zlotkin T, Farkash Y, Orly J.** Cell-specific expression of immunoreactive cholesterol side-chain cleavage cytochrome P-450 during follicular development in the rat ovary. *Endocrinology* 1986; **119**: 2809–2820. [Medline] [CrossRef]
23. **Magoffin DA, Weitsman SR.** Effect of insulin-like growth factor-I on cholesterol side-chain cleavage cytochrome P450 messenger ribonucleic acid expression in ovarian theca-interstitial cells stimulated to differentiate in vitro. *Mol Cell Endocrinol* 1993; **96**: 45–51. [Medline] [CrossRef]
24. **Hoang YD, McTavish KJ, Chang RJ, Shimasaki S.** Paracrine regulation of theca androgen production by granulosa cells in the ovary. *Fertil Steril* 2013; **100**: 561–567. [Medline] [CrossRef]
25. **Hillier SG, Yong EL, Illingworth PJ, Baird DT, Schwall RH, Mason AJ.** Effect of recombinant activin on androgen synthesis in cultured human thecal cells. *J Clin Endocrinol Metab* 1991; **72**: 1206–1211. [Medline] [CrossRef]
26. **Knight PG, Satchell L, Glister C.** Intra-ovarian roles of activins and inhibins. *Mol Cell Endocrinol* 2012; **359**: 53–65. [Medline] [CrossRef]
27. **M'baye M, Hua G, Khan HA, Yang L.** RNAi-mediated knockdown of INHBB increases apoptosis and inhibits steroidogenesis in mouse granulosa cells. *J Reprod Dev* 2015; **61**: 391–397. [Medline] [CrossRef]
28. **Hillier SG, Yong EL, Illingworth PJ, Baird DT, Schwall RH, Mason AJ.** Effect of recombinant inhibin on androgen synthesis in cultured human thecal cells. *Mol Cell Endocrinol* 1991; **75**: R1–R6. [Medline] [CrossRef]
29. **Magoffin DA, Kurtz KM, Erickson GF.** Insulin-like growth factor-I selectively stimulates cholesterol side-chain cleavage expression in ovarian theca-interstitial cells. *Mol Endocrinol* 1990; **4**: 489–496. [Medline] [CrossRef]
30. **Navarro VM, Castellano JM, Fernández-Fernández R, Barreiro ML, Roa J, Sanchez-Criado JE, Aguilar E, Dieguez C, Pinilla L, Tena-Sempere M.** Developmental and hormonally regulated messenger ribonucleic acid expression of KiSS-1 and its putative receptor, GPR54, in rat hypothalamus and potent luteinizing hormone-releasing activity of KiSS-1 peptide. *Endocrinology* 2004; **145**: 4565–4574. [Medline] [CrossRef]
31. **Gottsch ML, Cunningham MJ, Smith JT, Popa SM, Acohido BV, Crowley WF, Seminara S, Clifton DK, Steiner RA.** A role for kisspeptins in the regulation of gonadotropin secretion in the mouse. *Endocrinology* 2004; **145**: 4073–4077. [Medline] [CrossRef]